Nanostructures

Deutsche Ausgabe: DOI: 10.1002/ange.201503655
Internationale Ausgabe: DOI: 10.1002/anie.201503655

Rapid Cationization of Gold Nanoparticles by Two-Step Phase Transfer**

*Jukka Hassinen, Ville Liljeström, Mauri A. Kostiainen, and Robin H. A. Ras**

Abstract: *Cationic gold nanoparticles offer intriguing opportunities as drug carriers and building blocks for self-assembled systems. Despite major progress on gold nanoparticle research in general, the synthesis of cationic gold particles larger than 5 nm remains a major challenge, although these species would give a significantly larger plasmonic response compared to smaller cationic gold nanoparticles. Herein we present the first reported synthesis of cationic gold nanoparticles with tunable sizes between 8–20 nm, prepared by a rapid two-step phase-transfer protocol starting from simple citrate-capped particles. These cationic particles form ordered self-assembled structures with negatively charged biological components through electrostatic interactions.*

Among metallic nanoparticles, gold nanoparticles (AuNPs) have been most extensively studied because of their high stability and intriguing optical properties, dominated by the localized surface plasmon resonance (LSPR).[1–3] Their size, plasmonic properties, and functionalization possibilities, mean that they have potential in applications related to, for example, gene and drug delivery,[4–7] biodiagnostics,[7–9] detection of metal ions or biomolecules,[6–10] and imaging.[5,6] Importantly, the properties and possible applications of AuNPs strongly depend on their surface functionalization. Considering the vast amount of literature on AuNPs, there are relatively few reports on the preparation of cationic AuNPs,[11–17] even though they are interesting candidates especially for gene and drug delivery applications, as well as for various self-assembled structures where uniform size of building blocks is essential.[18,19] Thus, development of synthesis strategies for cationic AuNPs with excellent size control, colloidal stability, and narrow particle size distribution (PSD) is of high importance.

Previously, cationic AuNPs have been prepared mainly either by 1) directly reducing gold salts in presence of cationic ligands[11–17] or 2) through ligand exchange reactions or covalent linking of cationic ligands to AuNPs prepared by the Brust–Schiffrin method.[20–22] The size control and resulting particle monodispersity of the first method are typically poor, and the second method is limited to particle sizes of 5 nm or less, leading to only weak LSPR (Figure 1). Larger nanoparticles would offer stronger light absorption in the visible range because of the approximately cubic dependence of the LSPR intensity on particle size.[23] The strong and narrow LSPR absorption observed with large AuNPs would provide a more desirable starting point for applications such as AuNP-based sensing.

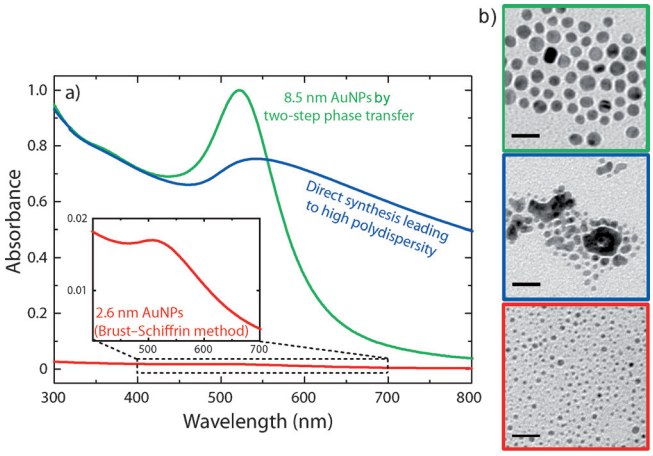

Figure 1. a) UV/Vis spectra of different cationic AuNPs: 2.6 nm (red; made by the Brust–Schiffrin method), 8.5 nm (green; made by two-step phase transfer), and polydisperse mixture (blue; made by direct synthesis). The molar nanoparticle concentration was adjusted to be the same for 2.6 and 8.5 nm AuNPs to illustrate the difference in their LSPR strength. b) Corresponding TEM images, scale bars: 20 nm.

One of the simplest methods to produce anionic AuNPs larger than 5 nm with a narrow PSD is the citrate reduction method, pioneered in 1951.[24] Citrate-AuNPs are straightforward to produce and their size can be tuned by varying the Au/citrate ratio,[25] reaction solution pH or temperature,[26] and by seeded growth approaches.[27] Citrate-AuNPs are tempting precursors for further functionalization efforts because of their fast, straightforward, and well-studied synthesis and high yield. For these reasons, citrate-AuNPs have been functionalized with stabilizing ligands including various amines[28] and thiols such as thiolated DNA,[29] polymers containing thiol or disulfide groups[30,31] and small thiol molecules, for example, mercaptosuccinic acid,[32] cysteine,[33] thioctic acid,[34] or hydrophobic thiols.[35] However, most of these systems produce negatively charged AuNPs because

[*] M. Sc. J. Hassinen, Prof. R. H. A. Ras
Department of Applied Physics, Aalto University
Puumiehenkuja 2, 02150 Espoo (Finland)
E-mail: robin.ras@aalto.fi
M. Sc. V. Liljeström, Prof. M. A. Kostiainen
Department of Biotechnology and Chemical Technology
Aalto University
Kemistintie 1, 02150 Espoo (Finland)

[**] This work was supported by the Academy of Finland through its Centres of Excellence Programme (2014–2019). The Aalto University Nanomicroscopy Center (Aalto-NMC) premises were utilized in this work.

Supporting information for this article is available on the WWW under http://dx.doi.org/10.1002/anie.201503655.

direct functionalization with a positively charged ligand typically leads to unwanted aggregation of AuNPs because of the detrimental electrostatic attraction between the ligands (Figure S1 in the Supporting Information).

We present herein the first reported synthesis of cationic gold nanoparticles with tunable size between 8–20 nm and narrow size distribution. The procedure involves a simple and rapid two-step phase transfer utilizing amine and thiol ligands. The resulting AuNPs are protected by thiols carrying quaternary ammonium groups making the AuNPs positively charged over a wide pH range. The two-step functionalization can be performed directly after the synthesis of citrate-AuNPs, is scalable, and the whole cationization process can be completed in less than an hour. To demonstrate their potential to efficiently bind large biomolecules and act as building blocks for nanoscale assemblies, we show that the cationic AuNPs readily interact with negatively charged virus particles and pack into ordered assemblies.

Five different sizes of citrate-AuNPs (Batches 1–5) were synthesized according to a modified Turkevich method (see the Supporting information).[27] The citrate-AuNPs were cationized by a two-step phase-transfer procedure shown in Figure 2. Citrate-AuNPs (30 mL) were transferred to toluene

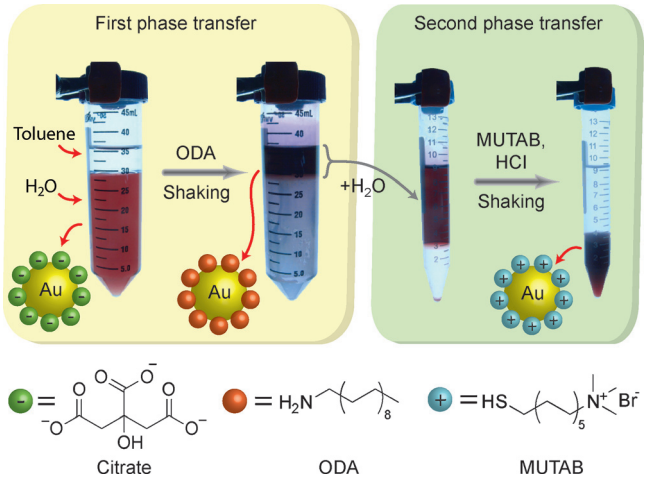

Figure 2. Two-step phase transfer of anionic citrate-AuNPs to cationic MUTAB-AuNPs via neutral ODA-AuNPs.

(6 mL) by adding octadecylamine (ODA; 5 μmol) and by shaking the two-phase mixture vigorously. The colored organic phase was separated and washed with water to remove any remaining citrate ions. Thereafter, water (3 mL) and (11-mercaptoundecyl)-*N*,*N*,*N*-trimethylammonium bromide (MUTAB; 300 μL; 4 mM in ethanol) were added to form a biphasic system and the tube was shaken to initiate the transfer of ODA-AuNPs to the aqueous phase. The transfer was completed by acidifying the mixture by addition of HCl, which causes protonation of ODA and thus detaches the remaining ODA molecules from the AuNP surface. Depending on the amount of excess ligands and the pH of the aqueous phase, ODA and MUTAB can act as surfactants, and occasionally an emulsion was formed. This gel-like material could be localized at the liquid–liquid interface by centrifugation and the aqueous phase could be easily collected. The aqueous phase was repeatedly washed with toluene to remove ODA and MUTAB residues. ^{1}H NMR spectroscopy was used to confirm the ligand compositions of amine- and thiol-protected AuNPs (Figure S2).

The amounts of ligands used in the procedure were optimized for the citrate-AuNP Batch 1 (see Figures S3 and S4). We found that the optimal ODA amount was 0.8 times the amount of Au atoms used in the synthesis. By evaluating the size of the AuNPs with transmission electron microscopy (TEM) and estimating the number of their surface atoms (see the Supporting information),[23] this ODA amount corresponds to roughly 5 times the amount of AuNP surface atoms. On the other hand, the amount of MUTAB was optimized to 0.25 times the amount of Au atoms which corresponds to roughly 1.75 times the amount of AuNP surface atoms. Importantly, this phase-transfer method allows an increase in the concentration of AuNPs during the cationization process by simply adjusting the volumes of the phases. An increase in concentration of over 30-fold can be easily realized when starting with a large volume of citrate-AuNPs (Figure S5). The MUTAB-AuNPs can be concentrated even further by centrifugation to reach concentrations over 20 mg mL^{-1}.

The cationization strategy is based on differences in Au–ligand interactions of citrate, amine, and thiol ligands. Citrate ligands are only electrostatically bound to the AuNP surface while the strength of interaction increases with amine ligand and increases further with thiol ligands, which form covalent Au–thiolate bonds. Importantly, a neutral amine (ODA) capping is utilized to avoid detrimental electrostatic interactions between the oppositely charged ligands. In addition to ODA, also the less expensive oleylamine can be utilized in the phase transfer.[36] It is worth noting that direct exchange of citrate to an alkanethiol in toluene causes an irreversible precipitation of AuNPs, thus making the intermediately strong, replaceable amine-capping indispensable (Figure S6). Finally, the thiolated MUTAB-AuNPs are highly stable and can be stored for months without noticeable aggregation. Analysis of the UV/Vis spectra of AuNP Batch 1 (Figure 3) shows that the LSPR maximum shifts only very slightly from citrate-AuNPs to MUTAB-AuNPs, thus suggesting that particle aggregation is negligible. Similar behavior is observed in all AuNP Batches 1–5 (Figure S7). The slight red-shift of the LSPR in MUTAB-AuNPs is suggested to arise from the change in the dielectric constant of the ligand layer. The red-shift is more prominent in ODA-AuNPs, and is enhanced by the higher refractive index of toluene compared to water.

A further simplification to the procedure is that it is not critical to pinpoint the exact amounts of ligands needed for the transfer. Incoming ligands can be gradually added and the completion of the transfer can be visually observed from the color of the phases (Figure 3b). The gradual addition of ligands reduces the final yield of the process only slightly (Figure S3b). It is also worth noting that the efficiency of the second phase-transfer step is affected by the material of the reaction vessel and thus should be carried out in a plastic vessel to avoid MUTAB-AuNPs sticking to the negatively charged glass walls. This two-step procedure was found to be

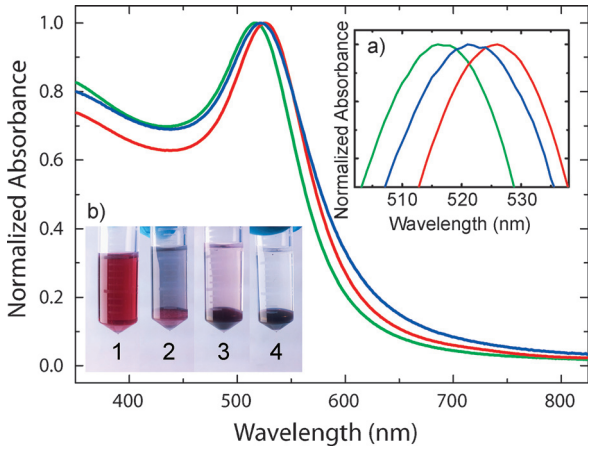

Figure 3. Typical UV/Vis spectra of AuNP Batch 1 during the phase transfer: citrate (green curve), ODA (red curve), and MUTAB (blue curve) capping. a) Close-up of the positions of the LSPR maxima. b) Photographs of a gradual transfer of ODA-NPs (1) to MUTAB-AuNPs. ODA-AuNPs are partially transferred to the H_2O phase by adding MUTAB (2). After addition of HCl, the phase transfer proceeds and reaches equilibrium (3). Second addition of MUTAB completes the phase transfer (4). See Figure S4B for additional details.

nearly quantitative for the smallest particles in this study (Batch 1, 8.5 nm). For larger particles, the typical yield was approximately 50–80%, with most loss occurring during the first phase-transfer step.

In addition to quaternized ammonium moieties, we have also prepared AuNPs functionalized with primary amines by using 6-aminohexanethiol hydrochloride (AHT) in the second exchange. In this case, the phase-transfer process was slower and was complete overnight. The UV/Vis spectrum of the AHT-AuNPs was comparable to the spectrum of MUTAB-AuNPs (Figure S8).

In order to further verify that the phase-transfer process does not change the size of the AuNPs, we imaged the particles before and after the cationization with TEM and determined the PSDs (Figure 4 and Figure S9 in the Supporting Information). As seen from the PSDs, there are no changes in the particle core sizes in Batches 1–3. The PSD in Batch 4 becomes slightly narrower in the cationization process. In order to probe the upper particle size limit of the procedure, the citrate-AuNPs from Batch 5 were deliberately synthesized to have a wider PSD ranging from 15 to 28 nm. As seen from the PSD data from Batch 5, the efficiency of the phase transfer drops substantially above 20 nm. Based on the visual observations during the phase-transfer experiments, most of the particle loss arises from aggregation during the first transfer from citrate-AuNPs to ODA-AuNPs. Thus, citrate-AuNPs larger than 20 nm do not readily undergo the first phase transfer, likely because of the lower curvature of the larger particles leading to poorly protected and easily aggregating AuNP surfaces at the liquid–liquid interface.[28] Therefore, this procedure is not directly suitable for cationization of nanoparticles larger than 20 nm.

In addition to TEM, dynamic light scattering (DLS) was also used to analyze the PSDs (Figure 3). For citrate-AuNPs, the average hydrodynamic diameters (D_h) were 2–3 nm larger than the average core diameter (D_{core}) measured by TEM. Similarly, the difference between D_{core} and D_h in MUTAB-AuNPs was 4–6 nm. These changes in D_h reflect the sizes of the ligands and are thus consistent with the D_{core} values obtained by TEM.

We also investigated the zeta potentials (ζ) of AuNPs with DLS. As expected, the average zeta potentials of the citrate-AuNPs were negative and ranged from −42.8 to −72.6 mV,

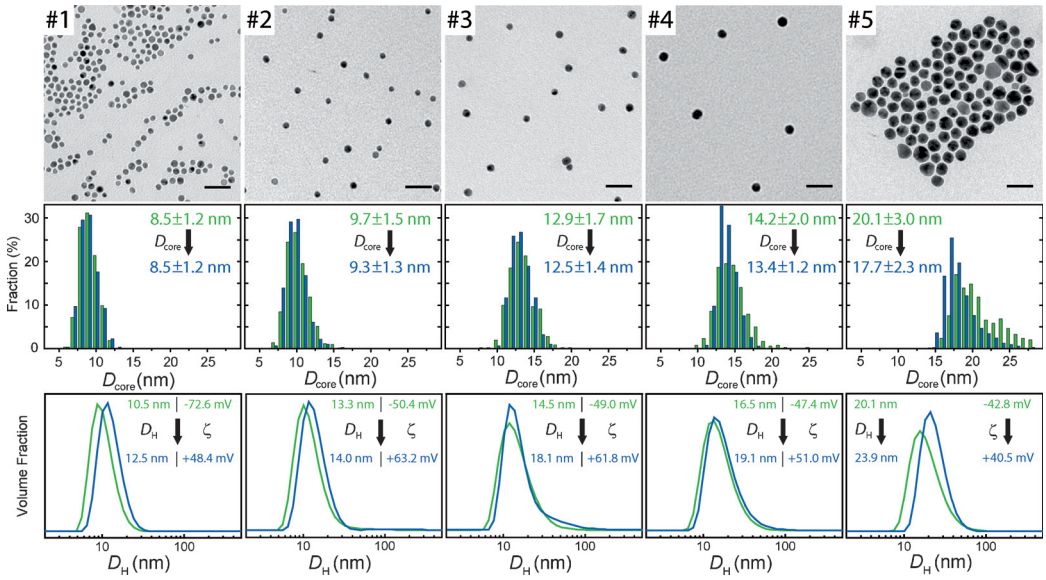

Figure 4. Above: TEM images of MUTAB-AuNP Batches 1–5. Scale bars: 40 nm. Center: Corresponding particle core size distributions (bin size 1 nm, $N_{AuNP} > 500$) based on TEM images of MUTAB-AuNPs (blue columns) and citrate-AuNPs (green columns). Average particle core sizes before and after cationization are shown. Below: Corresponding hydrodynamic particle diameter distributions measured with DLS of MUTAB-AuNPs (blue traces) and citrate-AuNPs (green traces). Hydrodynamic diameters and zeta potentials of AuNPs before and after cationization are shown.

slightly depending on the particle size. In contrast, the average zeta potentials of MUTAB-AuNPs were positive and varied from +40.5 to +63.2 mV, thus indicating a successful cationization of AuNPs. The zeta potential distributions of AuNP Batches 1–5 are given in Figure S10. The high zeta potential values are superior to previously reported values from +5 to +45 mV,[13,16,37] and ensure a high colloidal stability of MUTAB-AuNPs. The results are summarized in Table S1.

To verify the application potential in biological systems, the colloidal stability of MUTAB-AuNPs was tested in 10 mM phosphate buffered saline (PBS). No change in the LSPR was observed during 20 h incubation indicating high colloidal stability (Figure S11). In order to utilize this high stability and to demonstrate the potential of these particles to bind biologically relevant macromolecules, we prepared biotemplated electrostatic self-assembled systems of MUTAB-AuNPs by combining them with the cowpea chlorotic mottle virus (CCMV) particles. The oppositely charged particles rapidly self-assembled to generate visible complexes in less than 10 min. The structure of the colloidal assemblies was further characterized by using small-angle X-ray scattering (Figure S12), which indicated the formation of a AB_3 face-centered-cubic (fcc) structure, in contrast with the AB_8 crystal structure observed with smaller 2.6 nm cationic AuNPs in an earlier study.[19] Here, the use of large (>8 nm) cationic AuNPs allows the preparation of complexes with hybridized nanoparticle plasmon modes, which have previously been inaccessible with small AuNPs.

In conclusion, we have developed a facile, rapid, and scalable cationization strategy for gold nanoparticles of sizes from 8 to 20 nm using simple citrate-AuNPs as precursors. Cationic nanoparticles in this size range are interesting candidates for applications related to plasmon enhancement and for building blocks in biohybrid assemblies.

Keywords: gold · nanoparticles · phase transfer · self-assembly · surface plasmon resonance

How to cite: *Angew. Chem. Int. Ed.* **2015**, *54*, 7990–7993
Angew. Chem. **2015**, *127*, 8101–8104

[1] S. Link, M. A. El-Sayed, *Int. Rev. Phys. Chem.* **2000**, *19*, 409–453.
[2] P. Zhao, N. Li, D. Astruc, *Coord. Chem. Rev.* **2013**, *257*, 638–665.
[3] P. K. Jain, X. Huang, I. H. El-Sayed, M. A. El-Sayed, *Acc. Chem. Res.* **2008**, *41*, 1578–1586.
[4] I. Fratoddi, I. Venditti, C. Cametti, M. V. Russo, *J. Mater. Chem. B* **2014**, *2*, 4204–4220.
[5] D. A. Giljohann, D. S. Seferos, W. L. Daniel, M. D. Massich, P. C. Patel, C. A. Mirkin, *Angew. Chem. Int. Ed.* **2010**, *49*, 3280–3294; *Angew. Chem.* **2010**, *122*, 3352–3366.
[6] R. A. Sperling, P. R. Gil, F. Zhang, M. Zanella, W. J. Parak, *Chem. Soc. Rev.* **2008**, *37*, 1896–1908.
[7] E. Boisselier, D. Astruc, *Chem. Soc. Rev.* **2009**, *38*, 1759–1782.
[8] K. Saha, S. S. Agasti, C. Kim, X. Li, V. M. Rotello, *Chem. Rev.* **2012**, *112*, 2739–2779.
[9] N. L. Rosi, C. A. Mirkin, *Chem. Rev.* **2005**, *105*, 1547–1562.
[10] D. Liu, Z. Wang, X. Jiang, *Nanoscale* **2011**, *3*, 1421–1433.
[11] T. Li, D. Li, L. Zhang, G. Li, E. Wang, *Biomaterials* **2008**, *29*, 3617–3624.
[12] T. Niidome, K. Nakashima, H. Takahashi, Y. Niidome, *Chem. Commun.* **2004**, 1978–1979.
[13] B. Nikoobakht, M. A. El-Sayed, *Langmuir* **2001**, *17*, 6368–6374.
[14] R. Sardar, J.-W. Park, J. S. Shumaker-Parry, *Langmuir* **2007**, *23*, 11883–11889.
[15] M. Thomas, A. Klibanov, *Proc. Natl. Acad. Sci. USA* **2003**, *100*, 9138–9143.
[16] T. J. Cho, R. I. MacCuspie, J. Gigault, J. M. Gorham, J. T. Elliott, V. A. Hackley, *Langmuir* **2014**, *30*, 3883–3893.
[17] C. Subramaniam, R. T. Tom, T. Pradeep, *J. Nanopart. Res.* **2005**, *7*, 209–217.
[18] A. M. Kalsin, M. Fialkowski, M. Paszewski, S. K. Smoukov, K. J. M. Bishop, B. A. Grzybowski, *Science* **2006**, *312*, 420–424.
[19] M. A. Kostiainen, P. Hiekkataipale, A. Laiho, V. Lemieux, J. Seitsonen, J. Ruokolainen, P. Ceci, *Nat. Nanotechnol.* **2013**, *8*, 52–56.
[20] C. M. McIntosh, E. A. Esposito, A. K. Boal, J. M. Simard, C. T. Martin, V. M. Rotello, *J. Am. Chem. Soc.* **2001**, *123*, 7626–7629.
[21] K. K. Sandhu, C. M. McIntosh, J. M. Simard, S. W. Smith, V. M. Rotello, *Bioconjugate Chem.* **2002**, *13*, 3–6.
[22] C. Geidel, S. Schmachtel, A. Riedinger, C. Pfeiffer, K. Müllen, M. Klapper, W. J. Parak, *Small* **2011**, *7*, 2929–2934.
[23] X. Liu, M. Atwater, J. Wang, Q. Huo, *Colloids Surf. B* **2007**, *58*, 3–7.
[24] J. Turkevich, J. Hillier, P. C. Stevenson, *Discuss. Faraday Soc.* **1951**, *11*, 55.
[25] G. Frens, *Nat. Phys. Sci.* **1973**, *241*, 20–22.
[26] X. Ji, X. Song, J. Li, Y. Bai, W. Yang, X. Peng, *J. Am. Chem. Soc.* **2007**, *129*, 13939–13948.
[27] N. G. Bastús, J. Comenge, V. Puntes, *Langmuir* **2011**, *27*, 11098–11105.
[28] M. Karg, N. Schelero, C. Oppel, M. Gradzielski, T. Hellweg, R. von Klitzing, *Chem. Eur. J.* **2011**, *17*, 4648–4654.
[29] X. Zhang, M. R. Servos, J. Liu, *J. Am. Chem. Soc.* **2012**, *134*, 7266–7269.
[30] C. Mangeney, F. Ferrage, I. Aujard, V. Marchi-Artzner, L. Jullien, O. Ouari, E. D. Rékaí, A. Laschewsky, I. Vikholm, J. W. Sadowski, *J. Am. Chem. Soc.* **2002**, *124*, 5811–5821.
[31] J. S. Kang, T. A. Taton, *Langmuir* **2012**, *28*, 16751–16760.
[32] T. Zhu, K. Vasilev, M. Kreiter, S. Mittler, W. Knoll, *Langmuir* **2003**, *19*, 9518–9525.
[33] A. Majzik, L. Fülöp, E. Csapó, F. Bogár, T. Martinek, B. Penke, G. Bíró, I. Dékány, *Colloids Surf. B* **2010**, *81*, 235–241.
[34] S.-Y. Lin, Y.-T. Tsai, C.-C. Chen, C.-M. Lin, C.-H. Chen, *J. Phys. Chem. C* **2004**, *108*, 2134–2139.
[35] D. Baranov, E. N. Kadnikova, *J. Mater. Chem.* **2011**, *21*, 6152–6157.
[36] S. Mourdikoudis, L. M. Liz-Marzán, *Chem. Mater.* **2013**, *25*, 1465–1476.
[37] I. Ojea-Jiménez, L. García-Fernández, J. Lorenzo, V. F. Puntes, *ACS Nano* **2012**, *6*, 7692–7702.

Received: April 21, 2015
Published online: May 26, 2015

